DNA Sequence Recognition by Bispyrazinonaphthalimides Antitumor Agents†

Carolina Carrasco,‡ Alexandra Joubert,‡ Christelle Tardy,‡ Nicolas Maestre,‡ Monica Cacho,§ Miguel F. Braña,§ and Christian Bailly*,‡

INSERM U-524 et Laboratoire de Pharmacologie Antitumorale du Centre Oscar Lambret, IRCL, 59045 Lille, France, and Departamento de CC Químicas, Facultad de CC Experimentales y de la Salud, Universidad San Pablo-CEU, Urb. Montepríncipe, Boadilla del Monte, 28668 Madrid, Spain

Received April 22, 2003; Revised Manuscript Received August 18, 2003

ABSTRACT: Bifunctional DNA intercalating agents have long attracted considerable attention as anticancer agents. One of the lead compounds in this category is the dimeric antitumor drug elinafide, composed of two tricyclic naphthalimide chromophores separated by an aminoalkyl linker chain optimally designed to permit bisintercalation of the drug into DNA. In an effort to optimize the DNA recognition capacity, different series of elinafide analogues have been prepared by extending the surface of the planar drug chromophore which is important for DNA sequence recognition. We report here a detailed investigation of the DNA sequence preference of three tetracyclic monomeric or dimeric pyrazinonaphthalimide derivatives. Melting temperature measurements and surface plasmon resonance (SPR) studies indicate that the dimerization of the tetracyclic planar chromophore considerably augments the affinity of the drug for DNA, polynucleotides, or hairpin oligonucleotides and promotes selective interaction with G·C sites. The $(CH_2)_2NH(CH_2)_3NH(CH_2)_2$ connector stabilizes the drug−DNA complexes. The methylation of the two nitrogen atoms of this linker chain reduces the binding affinity and increases the dissociation rates of the drug−DNA complexes by a factor of 10. DNase I footprinting experiments were used to investigate the sequence selectivity of the drugs, demonstrating highly preferential binding to G·C-rich sequences. It also served to select a high-affinity site encompassing the sequence 5′-GACGGCCAG which was then introduced into a biotin-labeled hairpin oligonucleotide to accurately measure the binding parameters by SPR. The affinity constant of the unmethylated dimer for this sequence is 500 times higher than that of the monomer compound and ∼10 times higher than that of the methylated dimer. The DNA groove accessibility was also probed with three related oligonucleotides carrying G → c^7G, G → I, and C → M substitutions. The level of drug binding to the two hairpin oligonucleotides containing 7-deazaguanine (c^7G) or 5-methylcytosine (M) residues is unchanged or only slightly reduced compared to that of the unmodified target. In contrast, incorporation of inosine (I) residues considerably decreases the extent of drug binding or even abolishes the interaction as is the case with the monomer. The pyrazinonaphthalimide derivatives are thus much more sensitive to the deletion of the exocyclic guanine 2-amino group exposed in the minor groove of the duplex than to the modification of the major groove elements. The complementary SPR footprinting methodology combining site selection and quantitative DNA affinity analysis constitutes a reliable method for dissecting the DNA sequence selectivity profile of reversible DNA binding small molecules.

The strategy that consists of dimerizing a DNA intercalating agent was initiated in the mid-1970s with the development of bisacridines connected by aminoalkyl linkers (*1*−*5*). Over the past 20 years, a great variety of dimeric DNA binders have been reported, and a few of them exhibited promising antitumor activities. This is particularly true for the bisimidazoacridone compound WMC26 (*6*, *7*) and bisanthracycline derivative WP631 (*8*−*11*), which both exhibit significant in vivo activities. This strategy remains attractive, and recently, Denny and co-workers have successfully developed series of symmetric dimeric molecules containing tricyclic rings (acridine, phenazine, and indenoquinoline) connected by carboxamide-type linkers (*12*−*15*). A few unsymmetrical dimers have also been synthesized and tested as potential anticancer drugs (*16*, *17*). But the most extensively studied subgroup of tumor active dimeric DNA binders are certainly the bisnaphthalimides, composed of two symmetric tricyclic units connected by an aminoalkyl linker. The lead compounds bisnafide (DMP-80) and elinafide (LU79553) (Figure 1) have reached clinical trials for the treatment of solid tumors (*18*−*21*). DNA binding is believed to be pivotal for these two molecules to exert their anticancer activity. Bisnafide is a potent DNA binder, but this compound

† This work was supported by grants (to C.B.) from the Ligue Nationale Contre le Cancer (Equipe labellisée LA LIGUE) and (to M.C.) from Fundacion Ramon Areces and the DEGS (MEC-Spain, Grant PB98-0055) and the Universidad San Pablo-CEU (Grant 5-99/00 U.S.P.). This research has been supported by a Marie Curie Fellowship of the European Community Program "Improving Human Research Potential and the Socio-economic Knowledge Base" under Contract HPMFCT-2000-00701 (to C.C.).

* To whom correspondence should be addressed: INSERM U-524, IRCL, Place de Verdun, 59045 Lille, France. E-mail: bailly@lille.inserm.fr.

‡ INSERM U-524.

§ Universidad San Pablo-CEU.

10.1021/bi034637h CCC: $25.00
Published on Web 09/18/2003

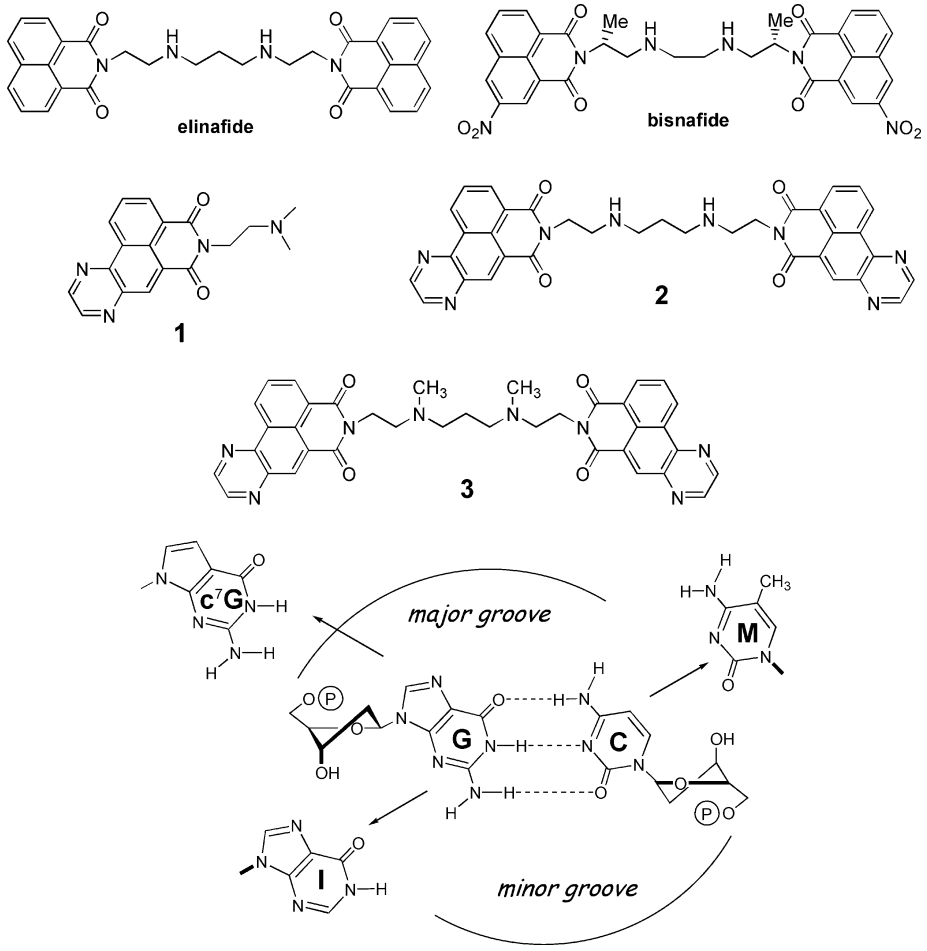

FIGURE 1: Structures of the drugs mentioned in this study and G·C base pairs with the modified bases inosine (I), 5-methylcytosine (M), and 7-deazaguanine (c^7G). Dashed lines represent hydrogen bonds. The sides of the base pair pointing into the major and minor grooves of the DNA double helix are indicated.

has appeared to be only a monointercalator (*22*). The capacity to inhibit topoisomerase II is responsible for its cytotoxicity (*23*). DNA and associated proteins are key elements of its mechanism of anticancer action (*24*−*28*). In contrast, elinafide exhibits a weaker capacity to inhibit topoisomerase II than bisnafide, but it forms true bisintercalation complexes. The propensity of elinafide to bisintercalate into duplex DNA has been firmly established on the basis of viscometric (*29*) and NMR data (*30*). The aminoalkyl linker chain connecting the two naphthalimide units resides in the major groove of DNA to establish molecular contacts with G·C base pairs.

In contrast to proteins, small molecules generally utilize the minor groove of DNA to interact with the DNA base pairs (*31*). Only a few drugs have been shown to be able to read the genetic information via the major groove of the DNA double helix. This is the case for elinafide but also for a few other polyfunctional molecules such as ditercalinium (*32*, *33*) and certain naphthalene diimides (*34*, *35*). The interesting antitumor profile of elinafide coupled with its unusual capacity to engage in contacts with the DNA major groove has stimulated the design of analogues capable of interacting with specific sites in DNA and susceptible to controlling the activity of cancer-related genes (*36*−*38*). The drug design strategy consists of preserving the aminoalkyl linker chain found in elinafide and substituting the two tricyclic naphthalimide chromophores for tetracyclic systems susceptible to reinforcing the DNA binding capacity, via better stacking and/or via direct H-bonding with the base pairs. The $(CH_2)_2NH(CH_2)_3NH(CH_2)_2$ linker chain separating the two chromophores by a distance of ∼12.3 Å [N−N distance for the fully extended form estimated by computer modeling (*14*)] is sufficient to allow both moieties to intercalate into DNA (*29*). An interchromophore separation of 9−13 Å is usually considered necessary to permit two planar ring systems to sandwich two base pairs in the intercalated complex (*39*). The naphthalimide unit has been fused to a benzene ring (*40*−*42*), an imidazole (*43*), a furan (*44*), a thiophene, or a pyrazine ring. The pyrazinonaphthalimide derivatives have revealed promising cytotoxic activities, and preliminary studies indicated that DNA binding plays a role in their cytotoxic action (*45*). Viscometry studies indicated that the bispirazinonaphthalimide derivative **2** behaves as a typical bisintercalating agent but does not inhibit human topoisomerases, despite its very strong cytotoxic action. To better comprehend its mechanism of action, we undertook the study reported here aimed at comparing the sequence selectivity of this dimeric molecule with that of two related compounds, the monomer **1** and the N-methylated dimer **3**.

MATERIALS AND METHODS

Drugs. The synthesis of the three pyrazinonaphthalimides has recently been described (*45*). The drugs (all three as methanesulfonate salts) were directly dissolved in water. The

stock solutions of drugs were kept at −20 °C and freshly diluted to the desired concentration immediately prior to use.

Melting Temperature Measurements. Melting curves were measured using a Uvikon 943 spectrophotometer coupled to a Neslab RTE111 cryostat. For each series of measurements, 12 samples were placed in a thermostatically controlled cell holder, and the quartz cuvettes (path length of 10 mm) were heated with circulating water. Measurements were performed in BPE buffer at pH 7.1 (6 mM Na_2HPO_4, 2 mM NaH_2PO_4, and 1 mM EDTA). The temperature inside the cuvette was measured with a platinum probe; it was increased over the range of 20−100 °C with a heating rate of 1 °C/min. The "melting" temperature T_m was taken to be the midpoint of the hyperchromic transition.

Immobilization of DNA and Surface Plasmon Resonance. Six 5′-biotin-labeled DNA hairpins (Eurogentec, PAGE-purified) were used in surface plasmon resonance studies (hairpin loop underlined): d(biotin-CATATATATCCCC-ATATATATG), d(biotin-CGCGCGCGTTTTCGCGCGCG), and d(biotin-GACGGCCAGTTTTCTGGCCGTC). Three analogues of the latter sequence with G → c^7G, C → M, and G → I substitutions were also used. Samples of hairpin DNA oligomers in HBS-EP buffer at 25 nM were applied to flow cells in streptavidin-derivatized sensor chips (BIAcore SA chips) by direct flow at 2 μL/min in a four-channel BIAcore 3000 optical biosensor system. HBS-EP buffer (BIA Certified) from BIACORE contains 0.01 M HEPES [*N*-(2-hydroxyethyl)piperazine-*N*′-2-ethanesulfonic acid], 0.15 M NaCl, 3 mM EDTA, and 0.005% polysorbate 20 (v/v) (pH 7.4). The sensor chips were conditioned with four consecutive 1 min injections of 1 M NaCl in 50 mM NaOH and three consecutive 15 s injections of 0.1% SDS in 3.5 mM EDTA, followed by extensive washing with buffer. Nearly the same amounts of all oligomers were immobilized on the surface by noncovalent capture, leaving one of the flow cells blank as a control. Manual injection was used with a flow rate of 2 μL/min to achieve long contact times with the surface and to control the amount of DNA bound to the surface. All procedures for binding studies were automated as methods using repetitive cycles of sample injection and regeneration. Steady-state binding analysis was performed with multiple injections of different compound concentrations over the immobilized DNA surfaces for a 15 min period at a flow rate of 20 μL/min and 25 °C. Solutions with known drug concentrations from 1.5 nM to 1.5 μM were prepared in filtered and degassed buffer by serial dilutions from a stock solution and were injected from 7 mm plastic vials with pierceable plastic crimp caps (BIAcore Inc.). In all cases, the DNA surface was regenerated by buffer flow over the course of 30 min without additional regeneration agents.

The instrument response (RU) in the steady-state region is proportional to the amount of bound drug and was determined by linear averaging over a period of 80 s. The predicted maximum response per bound compound in the steady-state region (RU_{max}) is determined from the DNA molecular weight, the amount of DNA in the flow cell, the compound molecular weight, and the refractive index gradient ratio of the compound and DNA (*46*, *47*). In the case presented here, the observed RU values at high concentrations are greater than RU_{max}, pointing to there being several binding sites in these DNA sequences. The RU_{max} value is required to convert the observed response (RU) to the standard binding parameter *r* (moles of drug bound per mole of DNA hairpin) using the equation

$$r = RU/RU_{max}$$

Average fitting of the sensorgrams at the steady-state level was performed with the BIAevaluation 3.0 program. To obtain the affinity constants, the results from the steady-state region were fitted with a multiple-equivalent site model using Kaleidagraph for nonlinear least-squares optimization of the binding parameters with the following equation:

$$r = nKC_{free}/(1 + KC_{free})$$

where *K*, the microscopic binding constant, is one variable to fit, *r* represents the number of moles of bound compound per mole of DNA hairpin duplex (*48*), C_{free} is the concentration of the compound in equilibrium with the complex and is fixed by the concentration in the flow solution, and *n* is the number of compound binding sites on the DNA duplex and is the second variable to fit. The *r* values are calculated by the ratio RU/RU_{max}, where RU is the steady-state response at each concentration and RU_{max} is the predicted RU for binding of a single compound to the DNA in a flow cell. Global kinetic fits to the sensorgrams to obtain association and dissociation kinetics constants were carried out using BIAevaluation software and an equivalent site interaction model.

DNase I Footprinting. The 117 and 265 bp DNA fragments were prepared by 3′ ^{32}P end labeling of the *Eco*RI−*Pvu*II double digest of the pBS plasmid (Stratagene) using [α-^{32}P]dATP (Amersham, 3000 Ci/mmol) and AMV reverse transcriptase (Roche). The two 198 bp fragments were obtained from plasmids pMS1 and pMS2 (kindly provided by K. R. Fox, University of Southampton, Southampton, U.K.) after digestion with restriction enzymes *Hin*dIII and *Xba*I (*49*). In each case, the labeled digestion products were separated on a 6% polyacrylamide gel under nondenaturing conditions in TBE[1] buffer [89 mM Tris-borate (pH 8.3) and 1 mM EDTA]. After autoradiography, the requisite band of DNA was excised, crushed, and soaked in water overnight at 37 °C. This suspension was filtered through a Millipore 0.22 μm filter, and the DNA was precipitated with ethanol. Following washing with 70% ethanol and vacuum-drying of the precipitate, the labeled DNA was resuspended in 10 mM Tris (adjusted to pH 7.0) containing 10 mM NaCl.

Bovine pancreatic deoxyribonuclease I (DNase I, Sigma Chemical Co.) was stored as a 7200 units/mL solution in 20 mM NaCl, 2 mM $MgCl_2$, and 2 mM $MnCl_2$ (pH 8.0). The stock solution of DNase I was kept at −20 °C and freshly diluted to the desired concentration immediately prior to use. Footprinting experiments were performed essentially as previously described (*50*). Briefly, reactions were conducted in a total volume of 10 μL. Samples (3 μL) of the labeled DNA fragments were incubated with 5 μL of the buffered solution containing the ligand at the appropriate concentration. After incubation for 30 min at 37 °C to ensure equilibration of the binding reaction, the digestion was initiated by the addition of 2 μL of a DNase I solution whose concentration was adjusted to yield a final enzyme concen-

[1] Abbreviations: SPR, surface plasmon resonance; TBE, Tris-borate-EDTA.

Table 1: Variation in Melting Temperature (ΔT_m) and Cytotoxicity

compound	ΔT_m (°C)[a]	IC_{50} (nM)[b]
1	3.9	870
2	19.6	5.4
3	15.6	11.7

[a] T_m measurements were performed in BPE buffer at pH 7.1 (6 mM Na_2HPO_4, 2 mM NaH_2PO_4, and 1 mM EDTA) using 2 μM drug and 20 μM calf thymus DNA (nucleotide concentration) with a heating rate of 1 °C/min. [b] Drug concentration that inhibits CEM leukemia cell growth by 50% after incubation in liquid medium for 72 h.

tration of ~0.01 unit/mL in the reaction mixture. After 3 min, the reaction was stopped by freeze-drying the mixture. Samples were lyophilized and resuspended in 5 μL of an 80% formamide solution containing tracking dyes. The DNA samples were then heated at 90 °C for 4 min and chilled in ice for 4 min prior to electrophoresis.

DNA cleavage products were resolved by polyacrylamide gel electrophoresis under denaturing conditions (0.3 mm thick, 8% acrylamide containing 8 M urea). After electrophoresis (~2.5 h at 60 W, 1600 V in a Tris-Borate/EDTA buffered solution), gels were soaked in 10% acetic acid for 10 min, transferred to Whatman 3MM paper, and dried under vacuum at 80 °C. A Molecular Dynamics 425E PhosphorImager was used to collect data from the storage screens exposed to dried gels overnight at room temperature. Baseline-corrected scans were analyzed by integrating all the densities between two selected boundaries using ImageQuant version 3.3. Each resolved band was assigned to a particular bond within the DNA fragments by comparison of its position relative to sequencing standards generated by treatment of the DNA with dimethyl sulfate followed by piperidine-induced cleavage at the modified guanine bases in DNA (G-track).

RESULTS

General DNA Binding Considerations. Melting temperature (T_m) measurements were performed with calf thymus DNA. The ΔT_m values ($T_m^{\text{drug−DNA complex}} - T_m^{\text{DNA alone}}$) given in Table 1 provided the first line of evidence indicating that the dimeric molecules exhibit a higher affinity for DNA than does the monomeric compound **1**. Moreover, the lower ΔT_m value recorded with **3** compared to that of **2** already suggested that the methylation of the nitrogen atoms in the linker chain reduced the DNA binding affinity, and the SPR data reported below have fully confirmed this primary observation.

Surface Plasmon Resonance (SPR) To Differentiate Binding to A·T and G·C Sequences. Two DNA hairpin oligonucleotides containing either an $[A{\cdot}T]_4$ or a $[C{\cdot}G]_4$ tract were immobilized on a sensor chip via a biotin−streptavidin noncovalent coupling. The analyte (**1**, **2**, or **3**) in solution was passed to the nucleic acid receptor trapped onto the surface of the sensor chip, and the observed binding rates and binding levels were measured to provide information about the sequence selectivity, kinetics, and affinity of the interactions. This method, which exploits evanescent waves at the surface of the DNA-coated gold layer, has proven to be extremely powerful in measuring accurate binding parameters (*47*, *51*). Binding of each drug to the surface-immobilized DNA alters the refractive index of the medium near the surface, and this change, measured in real time, is directly proportional to the amount of bound drug molecules. By this sensitive method, binding affinities and kinetics can be determined accurately.

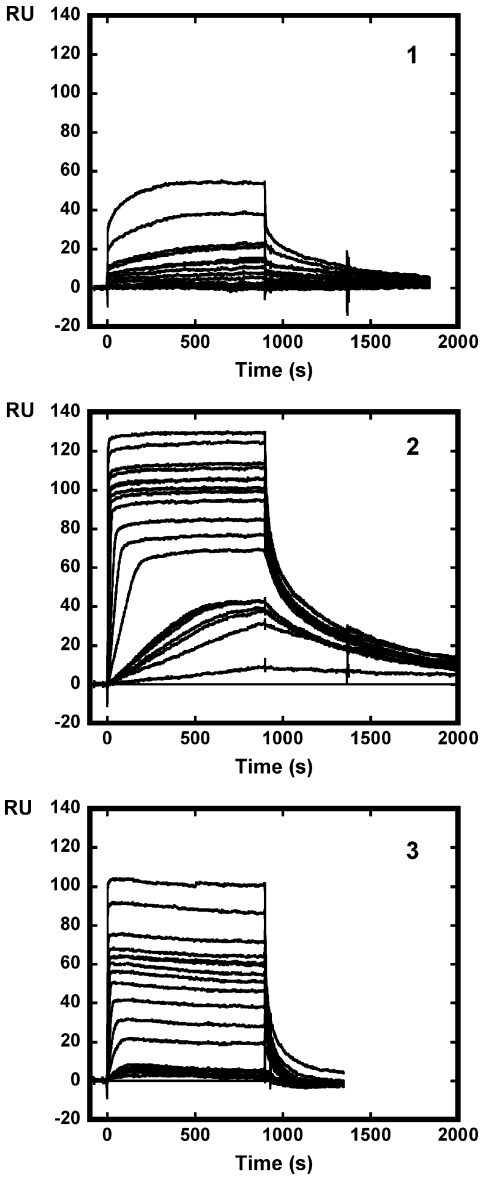

FIGURE 2: SPR sensorgrams for binding of **1** (top), **2** (middle), and **3** (bottom) to the $[C{\cdot}G]_4$ hairpin oligomer in HBS-EP buffer at 25 °C. The concentration of the unbound ligand in the flow solution varies from 1.5 nM in the bottom curve to 1.5 μM in the top curve.

A set of SPR sensorgrams (response units vs time) at different concentrations of **1**, **2**, or **3** binding to the $[C{\cdot}G]_4$ sequence is shown in Figure 2. As can be seen, the two dimeric molecules show much better interaction with the G·C site than the monomer. With the $[A{\cdot}T]_4$ sequence, the level of interaction was even more reduced, and in this case, binding of the monomeric compound was negligible (data not shown). One can immediately see that there are significant differences between the two dimeric compounds in terms of binding kinetics. The association and dissociation of the **3**−G·C complexes proceed much more rapidly than those with the nonmethylated dimer **2**. This latter compound exhibits a very high affinity for DNA, and the kinetics of the reactions were sufficiently slow to allow us to estimate

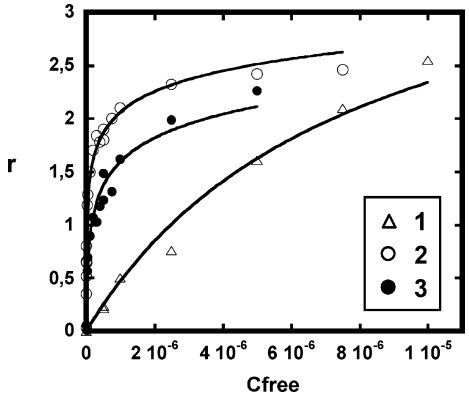

FIGURE 3: Binding plots (r vs C_{free}) used to determine the affinity constants for **1** (△), **2** (○), and **3** (●) complexed with the duplex $[C{\cdot}G]_4$ sequence. To construct these plots, RU values from the steady-state region of the SPR sensorgrams presented in Figure 2 were converted to r (moles of drug bound per mole of DNA hairpin) and plotted vs the concentration of unbound drug.

Table 2: Equilibrium Binding and Kinetic Constants for Drug Binding to the $[A{\cdot}T]_4$ and $[C{\cdot}G]_4$ Sequences[a]

compound	sequence	K_{eq} (M^{-1})	k_a ($M\ s^{-1}$)	k_d (s^{-1})	n
1	$[A{\cdot}T]_4$	4.71×10^4	*b*	*b*	8−10
	$[C{\cdot}G]_4$	9.77×10^4	*b*	*b*	3−4
2	$[A{\cdot}T]_4$	3.06×10^6	3.3×10^5	3.4×10^{-2}	3
	$[C{\cdot}G]_4$	4.6×10^7	2.22×10^5	2.48×10^{-3}	2
3	$[A{\cdot}T]_4$	1.36×10^6	*b*	*b*	2
	$[C{\cdot}G]_4$	4.61×10^6	4.48×10^5	2.9×10^{-2}	2

[a] Experiments were performed in HBS-EP buffer. [b] Association or dissociation too fast to be measured. The DNA sequences show one strand of the duplex stem of the hairpin used in the BIAcore SPR experiments. The number of compound binding sites on the DNA duplexes is given (n).

the association (k_a) and dissociation (k_d) parameters with both the A·T and G·C sequences (see below). With the two DNAs, binding affinities were determined from the steady-state plateau region of the sensorgrams. Typically, the raw RU data were converted to plots of r versus C_{free} and fit to determine the binding constants as described in Materials and Methods. Plots obtained with the G·C sequence are presented in Figure 3. The K_{eq} values are determined for each set of sensorgrams by nonlinear least-squares fitting of r versus C_{free} plots for the compound bound to the A·T or G·C DNA. The calculated binding parameters are listed in Table 2. The equilibrium binding constant K_{eq} measured with **2** is 470 times higher than that determined with **1**. This is a considerable gain in affinity which illustrates the contribution of the two pyrazinonaphthalimide units connected by a nonmethylated aminoalkyl linker. Surprisingly, methylation of the two nitrogen atoms in the linker chain reduces the level of binding to the G·C sequence by a factor of 10. The negative contribution of the methyl group is less marked at the A·T site but still observed (compare the K_{eq} values for **2** and **3**). The pyrazinonaphthalimide compounds bind significantly more tightly to the $[C{\cdot}G]_4$ sequence than to the $[A{\cdot}T]_4$ sequence. With **2**, The $K_{eq}^{G\cdot C}/K_{eq}^{A\cdot T}$ ratio amounts to 15, and this observation is in perfect agreement with the footprinting data reported below.

The analysis of the kinetic parameters also reveals marked differences between the methylated and nonmethylated dimers interacting with the $[C{\cdot}G]_4$ sequence. The NH compound **2** exhibits slower association and dissociation rates

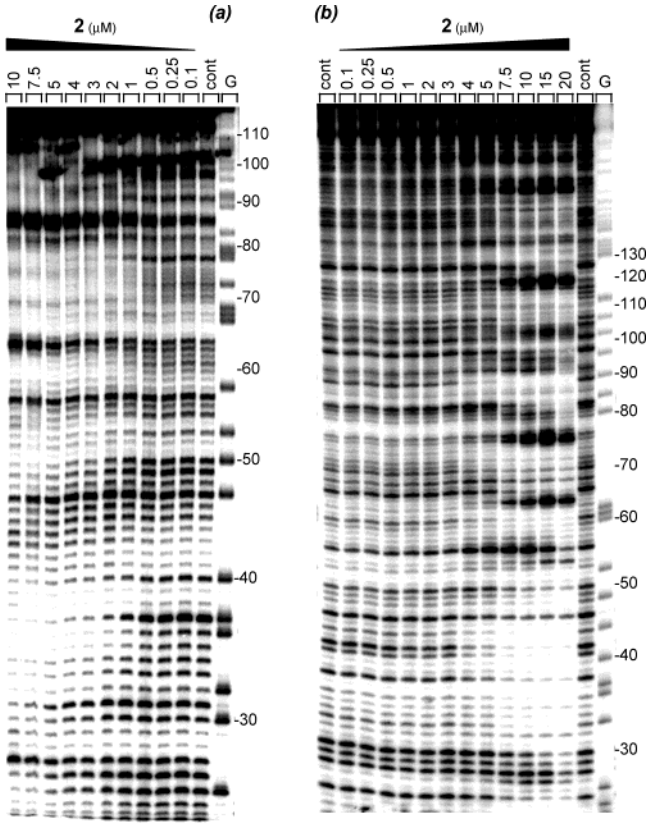

FIGURE 4: DNase I footprinting of pyrazinonaphthalimide **2** on the *Hin*dIII−*Xba*I 198 bp (a) MS1 and (b) MS2 fragments containing the cloned sequence with a combination of all 136 distinguishable tetranucleotide sequences. In each case, the DNA was 3′-end labeled with [α-^{32}P]dATP in the presence of AMV reverse transcriptase. The products of nuclease digestion were resolved on 8% polyacrylamide gels containing 7 M urea. Control tracks (cont) contained no drug. The concentration (micromolar) of the test drug is shown at the top of the appropriate gel lanes. Tracks labeled "G" represent dimethyl sulfate−piperidine markers specific for guanines. Numbers on the left side of the gels refer to the standard numbering scheme for the nucleotide sequence of the DNA fragment, as indicated in Figure 5.

than the *N*-Me analogue **3**. The difference is most pronounced at the dissociation level with a k_d that is ∼10 times lower with **2** than with **3**. The methylation of the linker nitrogens is detrimental to the temporal stability of the drug−DNA complexes. It is interesting to note also that the k_a values obtained with **2** binding to the A·T and G·C sequences are roughly similar whereas there is a significant difference at the dissociation level with a $k_d^{A\cdot T}/k_d^{C\cdot G}$ ratio of 13.7, suggesting therefore that the G·C selectivity inferred from the footprinting experiments (see below) arises from the longer residence of the ligand on the DNA at G·C sites.

Considering the length of the hairpin oligonucleotides and the size of the drug molecules, we can estimate that each DNA can offer approximately four monointercalation or two bisintercalation binding sites, and this prediction is consistent with the experimental observation, at least for the G·C sequence (n values in Table 2). Binding to the A·T sequence is less selective, and in this case, external binding may occur. High n values in the range of 8−10, as is the case for the binding of monomer **1** to the A·T sequence, must reflect the existence of a secondary binding mode, probably an external electrostatic interaction as we have observed with other cationic DNA ligands (*52*, *53*). The hairpin oligonucleo-

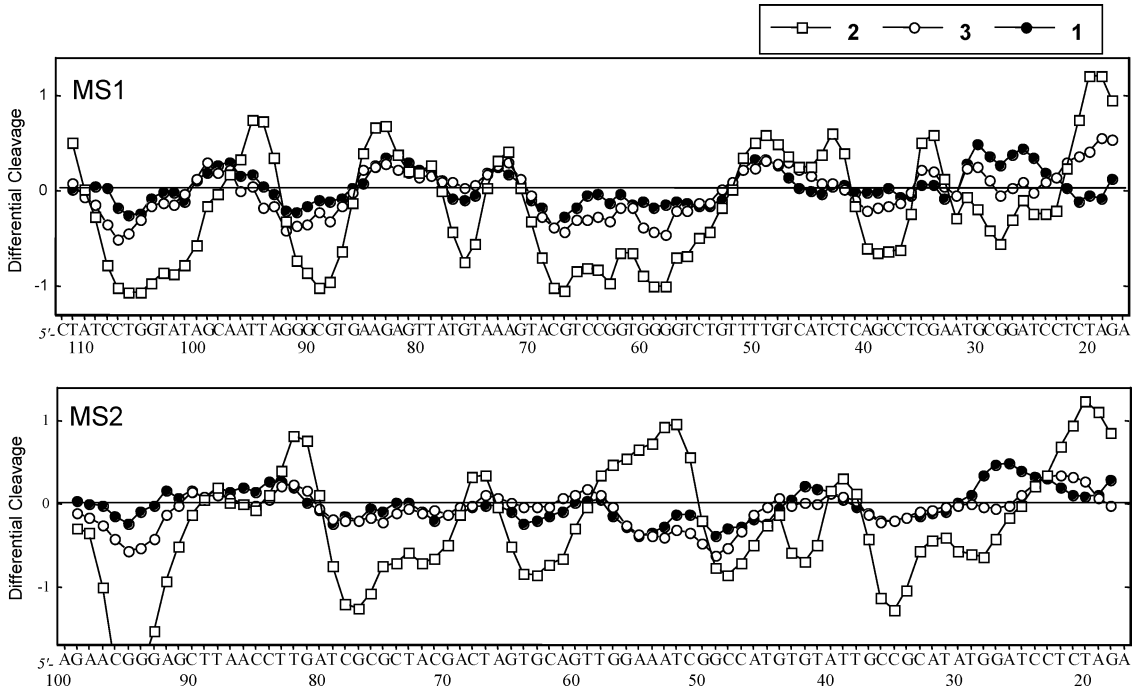

FIGURE 5: Differential cleavage plots comparing the susceptibility of the MS1 and MS2 fragments to DNase I cutting in the presence of the three pyrazinonaphthalimides (5 μM each). Negative values correspond to a ligand-protected site, and positive values represent enhanced cleavage. Vertical scales are in units of $\ln(f_a) - \ln(f_c)$, where f_a is the fractional cleavage at any bond in the presence of the drug and f_c is the fractional cleavage of the same bond in the control, given closely similar extents of overall digestion. Only the region of the restriction fragment analyzed by densitometry is shown.

tides easily accommodate two bispyrazinonaphthalimide molecules.

DNase I Footprinting To Characterize an Optimal Binding Site. Four DNA restriction fragments were prepared by 3′-end radiolabeling with ^{32}P: two fragments with random DNA sequences, 117-mer and 265-mer, both obtained from the plasmid pBS digsted with *Eco*RI and *Pvu*II, two designed fragments of 198 bp termed "universal footprinting substrates" (*49*) containing all 136 distinguishable tetranucleotide sequences ($4^4/2 + 4^{4/2}/2 = 136$). These two fragments, MS1 and MS2, contain the same sequence of 136 bp but cloned in the opposite orientation, 5′ → 3′ and 3′ → 5′. With each fragment, the products of digestion by DNase I in the absence and presence of the test drugs were resolved by polyacrylamide gel electrophoresis. DNase I digestion patterns of the MS1 and MS2 DNA fragments observed in the absence and presence of the bisnaphthalimide compound **2** are shown in Figure 4. Several sites are protected from DNase I cleavage by bisnaphthalimides **2** and **3**, whereas mononaphthalimide **1** showed little effect on the enzyme cutting. The modifications of the cleavage profiles are most pronounced with the nonmethylated dimer **2**, with several well-resolved sites of protection from DNase I cutting (footprints) adjacent to regions of enhanced cleavage. The gels were analyzed by phosphorimaging to determine the exact position of the footprints, presumptive ligand binding sites. A range of binding sequences were identified from differential cleavage plots (Figure 5). Compound **2** binds selectively to many sequences with a high G·C content, such as 5′-CCTGG, 5′-GGCG, 5′-CGTCCGGTGGG, 5′-AGCC, 5′-GCCGC, 5′-CGCGC, and 5′-CGGG. In a few cases, weaker binding to a few A·T/G·C mixed sequences, such as 5′-ATGT and 5′-TGGA, is also observed. On the other hand, DNase I cutting at A·T-rich sequences is significantly enhanced in the presence of **2**, and this effect can be attributed to intercalation-induced perturbations of the double-helical structure of DNA. Methylated dimer **3** and monomer **1** exhibit a reduced sequence selectivity, but they also bind better to the same G·C-rich sites as **2**, indicating therefore that the G·C preference arises from the intercalated pyrazinonaphthalimide ring rather than from the aminoalkyl linker chain.

With the 117-mer and the 265-mer, we also detected strong footprints with the nonmethylated dimer **2** (Figure S1). At a few sites, such as around position 40 in the 265-mer, the DNase I cleavage is totally inhibited so a true footprint is generated. With increasing concentrations of **2**, the involvement of a specific binding process becomes unambiguous as judged from the blockage of the enzyme activity at defined internucleotide bonds. The differential cleavage plots (Figure S2) show that compound **2** inhibits DNA cleavage at G·C-rich sites. The sequence 5′-CGGCC (positions 34−38 in the 117-mer) was identified as a highly favorable binding sequence for **2**. It also provides a receptor site for **3** and **1**, but the comparative analysis indicates that these two molecules interact much less tightly with this G·C-containing site than **2** (Figure 6). Among the various binding sites identified within the four DNA fragments used in footprinting experiments, this particular 5′-CGGCC sequence was chosen as the most favorable binding receptor and a biotin-labeled oligonucleotide corresponding to that sequence was prepared for subsequent SPR experiments.

SPR Analysis for Binding to a High-Affinity Site. Additional SPR experiments were performed with the 5′-biotinylated oligomer 5′-GACGGCCAGTTTTCTGGCCGTC (hairpin loop underlined) copied directly from the DNase I footprinting experiments (Figure 6). Solutions of **1**−**3** at increasing concentrations (from 1 nM to 5 μM) were passed over this hairpin duplex immobilized on a BIAcore SA sensor

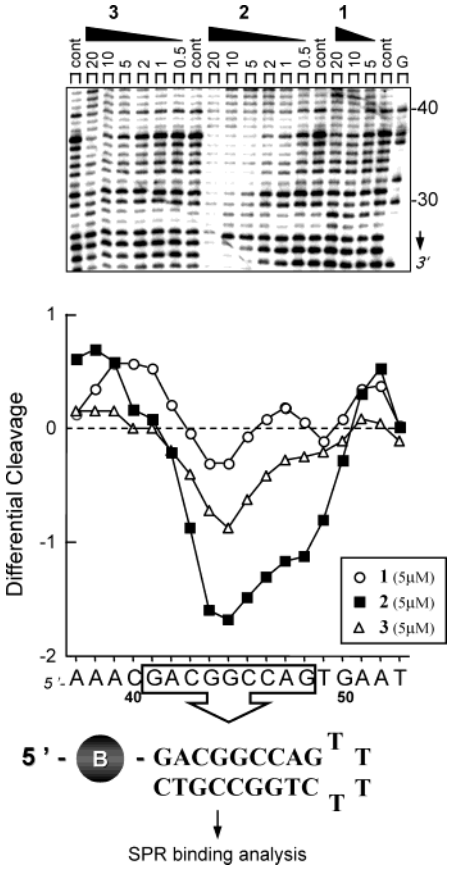

FIGURE 6: Illustration of the strategy developed to identify a high-affinity drug binding for SPR analysis. DNase I footprinting experiments with the 117 bp fragment define sequence protected from nuclease cleavage in the presence of the pyrazinonaphthalimides. This sequence was synthesized as a biotin-labeled (sphere marked with a B) oligomer hairpin and then used for the SPR experiments as shown in Figure 9.

chip (Figure 7). With the dimeric compounds, a steady-state response plateau was easily achieved at each concentration and averaged over 80 s to yield the RU values. The plateau value was more difficult to reach with the monomer because of the low binding affinity, but nevertheless in all cases, the affinity constants could be measured from the steady-state regions fitted with a one-site interaction model using the nonlinear least-squares optimization procedure. The equilibrium binding constants (Table 3) indicate that the affinity of **2** for the CGGCC-containing target sequence is considerably higher (~5000 times) than that of **1**. Compound **2** binds to this sequence ~10 times more tightly than **3**, reinforcing therefore the idea that the methylation of the linker chain is unfavorable for DNA recognition.

Three types of structural modifications were introduced into the CGGCC-containing high-affinity sequence: G → deazaG, G → I, and C → MeC substitutions. The use of hairpin oligonucleotides containing either 7-deazaguanine (c^7G), inosine (I), or 5-methylcytosine (M) residues permits identification of some of the factors which affect its DNA binding sequence selectivity. Sensorgrams obtained with each modified oligonucleotide are presented in Figure 7, and the binding constants extracted from these SPR experiments are given in Table 3. The SPR data were fitted satisfactorily with a one-site model for the monomeric compound **1**, and there was no improvement with a two-site interaction model. In contrast, the fitting of the SPR data collected with dimeric compounds **2** and **3** was slightly better when using the two-site model: $r = (n_1K_1C_{free})/(1 + K_1C_{free}) + (n_2K_2C_{free})/(1 + K_2C_{free})$. The K_1 and K_2 values collated in Table 3 for these two compounds are always much higher than the K_{eq} values measured with the corresponding monomer. Intuitively, one may suggest that K_1 reflects bisintercalative binding of the drugs to DNA, whereas K_2, which is always considerably lower than K_1 (up to 500 times), corresponds to a fraction of monointercalated molecules. In fact, the secondary binding mode is minimal because the K_1 values do not greatly differ from the K_{eq} values obtained with the one-site model and the low-drug concentration data set (data not shown).

With the monomer, the G → c^7G and C → M substitutions have little, if any, impact on the binding of the drug to DNA whereas the G → I substitution abolishes drug binding. A more or less similar situation was found with the dimeric molecules. The G → c^7G substitution reduces the level of binding of **2** to the target oligonucleotide by a factor of only 2, whereas the C → M substitution has absolutely no influence on drug binding. The effect of the major groove substitutions is more pronounced with the methylated molecule **3** since in this case the removal of the N7 atom on the guanine residues decreases the level of drug binding by a factor of 5.8. The methylated compound is also totally insensitive to the addition of a methyl group on the cytosine residue. In sharp contrast, the deletion of the guanine 2-amino group exposed in the minor groove has a major effect on the interaction of the two dimeric molecules with DNA. With both **2** and **3**, K_1 drops by a factor of 75−80 when inosines are substituted for guanosines. These experiments suggest that the guanine 2-amino group is a key element for tight binding of the bispyrazinonaphthalimides to the 5′-GACGGCCAG sequence.

An improper folding or denaturation of the inosine-containing oligonucleotide could account for the reduced level of binding of the pyrazinonaphthalimides. However, circular dichroism measurements indicated that under the experimental conditions used for the SPR measurements, the inosine oligonucleotide presents a B-type conformation similar to that of the G-containing parent oligonucleotide (Figure S3). Moreover, the minor groove binding drug netropsin was found to bind well to this inosine oligomer (data not shown), suggesting therefore that it is correctly folded. However, a slightly modified conformation cannot be excluded.

DISCUSSION

Oligonucleotides coated on a thin gold surface provide useful biosensor tools for investigating the molecular interaction of small molecules with nucleic acids, by means of the surface plasmon resonance phenomenon which measures changes in the refraction index near the metal surface. DNA-coated SPR chips have attracted considerable attention in recent years because it requires no radioactive labeling procedure and provides real time and quantitative analysis of the binding process. The sensor method is now well adapted to the study of drug−DNA interactions (*51*). Wilson and co-workers have extensively used SPR to analyze interaction of DNA and RNA oligonucleotides with different types of small molecules, in particular minor groove binders (*54*−*58*). The method is also appropriate for DNA intercalat-

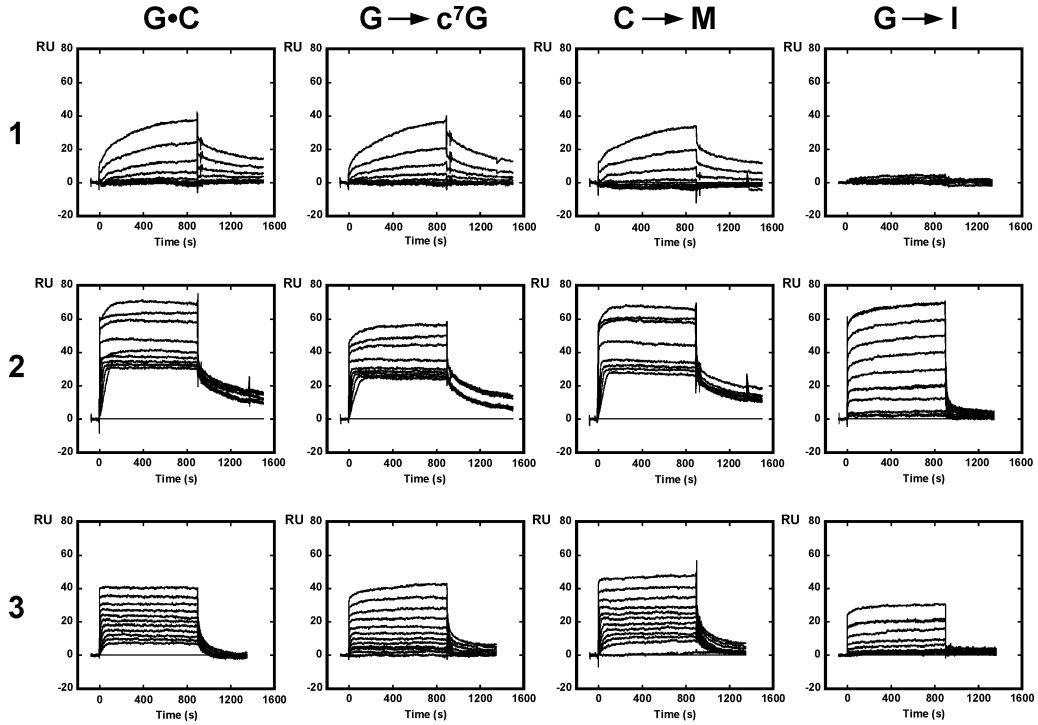

FIGURE 7: SPR sensorgrams for binding of **1** (top), **2** (middle), and **3** (bottom) to the high-affinity site selected from the footprinting experiments. The hairpin oligonucleotide d(GACGGCCAGTTTTCTGGCCGTC) (hairpin underlined) contained either normal bases or 7-deazaguanosine (G → c^7G substitution), 5-methylcytosine (C → M substitution), or inosine (G → I substitution) residues in place of guanosines, cytosines, and guanosines, respectively. Experiments were performed in HBS-EP buffer at 25 °C. The concentration of the unbound ligand in the flow solution varies from 1 nM in the bottom curve to 5 μM in the top curve.

Table 3: Binding Constants for Drug Interaction with the d(GACGGCCAGTTTTCTGGCCGTC) Sequence and Its Analogues Containing Modified Bases[a]

hairpin oligonucleotide	**1**		**2**		**3**	
	K_{eq} (M^{-1})	*n*	K_1, K_2 (M^{-1})	*n*	K_1, K_2 (M^{-1})	*n*
G•C	2.40×10^5	4	$K_1 = 1.18 \times 10^9$ $K_2 = 2.93 \times 10^6$	1 + 1	$K_1 = 9.12 \times 10^7$ $K_2 = 3.77 \times 10^5$	1 + 1
G → c^7G	1.35×10^5	5	$K_1 = 4.99 \times 10^8$ $K_2 = 6.85 \times 10^5$	1 + 1	$K_1 = 1.56 \times 10^7$ $K_2 = 3.98 \times 10^5$	1 + 1
C → M	1.74×10^5	4	$K_1 = 1.39 \times 10^9$ $K_2 = 2.56 \times 10^6$	1 + 1	$K_1 = 1.04 \times 10^8$ $K_2 = 6.77 \times 10^5$	1 + 1
G → I	–	–	$K_1 = 1.55 \times 10^7$ $K_2 = 1.03 \times 10^6$	1 + 1	$K_1 = 1.09 \times 10^6$ $K_2 = 1.04 \times 10^5$	1 + 1

[a] Experiments were performed in HBS-EP buffer. The hairpin oligonucleotides contained either conventional G•C base pairs, inosines (I), or 7-deazaguanines (c^7G) in place of guanines, or 5-methylcytosine (M) in place of cytosines. The number of compound binding sites on the DNA duplexes is given (*n*).

ing drugs (e.g., indolocarbazoles and acridines) (*53*, *59*), and more recently, we used it to probe the interaction of dimeric drugs with quadruplex DNA structures (ditercalinium and bisbenzophenanthroline) (*60*, *61*). The SPR technology has proven also to be very useful in dissecting the biomolecular interaction of the bisnaphthalimide family of anticancer agents. We started with a bisfuranonaphthalimide derivative (*44*), and we have now extended the analysis to bispyrazinonaphthalimides **2** and **3**. Therefore, a large range of binding agents, all representing low-molecular weight analytes, have been successfully tested for DNA binding by SPR which complements the panoply of biophysical techniques available for dissection of drug−nucleic acid interactions.

This study of the mono- and bispyrazinonaphthalimides raises several important questions. First, it confirms the utility of the SPR technique in quantifying drug−DNA interactions, in particular, for tight DNA binders with K_{eq} values approaching 10^{10} M^{-1}. Second, the study highlights the power of the combined footprinting−surface plasmon resonance (FP−SPR) approach in identifying optimized binding sites and evaluating the binding parameters accurately. SPR is convenient for analyzing drug binding to a short sequence containing generally one or at most three to four closely spaced sites, but this biophysical technique is not well-suited for selection of recognition sites. In contrast, footprinting is the method of choice for site selection, but quantification of drug−DNA interaction by this biochemical technique is laborious and relatively inaccurate. The combined FP−SPR strategy, as reported here and in two recent studies (*53*, *54*), is very promising as it associates site selection with quantification (and eventually kinetics). It is likely that the FP−SPR tango will become a favorite practice in studying drug−nucleic acid interactions. Third, and for the first time, we made profit of the versatility of nucleotide synthesis to incorporate modified bases into biotin-labeled DNA oligonuleotides, and we used these DNA substrates to dissect the

recognition process. The use of specific bases with additional exocyclic groups or lacking H bond donor or acceptor groups found in the canonical bases is interesting in identifying molecular determinants involved in the drug−DNA recognition process.

Beyond the methodological aspect discussed above, the purpose of this work was to comprehend further the interaction of modified bisnaphthalimides with DNA. The antitumor drug elinafide, with its two tricyclic naphthalimide units connected by a 12 Å long aminoalkyl linker, has been used as a platform to introduce functionality which may reinforce DNA interaction and confer different sequence selectivity. Many different types of structural modifications have been considered in the past years: variation of the length and flexibility of the linker and changes in the chromophore. But lately we focused on the incorporation of a fourth heterocycle fused to the naphthalimide core. The goal was to enhance the surface of the chromophore to facilitate stacking interaction and to incorporate H bond donor or acceptor heteroatoms to facilitate base pair contacts. Imidazonaphthalimides were first reported (*43*), and we recently evaluated furanonaphthalimides (*44*) prior to focusing on the pyrazinonaphthalimide derivatives. As mentioned in the introductory section, pyrazinonaphthalimide dimers **2** and **3** have been identified as potent cytotoxic agents (*45*). For information, a series of IC_{50} values (drug concentration to inhibit cell growth by 50%) are indicated in Table 1. The fact that the monomer is much less cytotoxic than the dimers suggests that DNA binding plays a role in the cytotoxic action. The tighter the binding, the more efficient the inhibition of cell growth. This simple rule is often observed in the naphthalimide series; however, we all know that DNA binding is not sufficient to explain cytotoxicity. DNA topoisomerases have been initially proposed as targets for certain bisnaphthalimides, but our recent study indicated that neither the furano- nor the pyrazinonaphthalimides stimulate topoisomerase I/II-mediated DNA cleavage (*44*, *45*). A few DNA-binding proteins, in particular, transcription factors, are currently being studied to determine if they can represent targets for these compounds.

The three compounds studied here exhibit a very different affinity for DNA. Monomer **1** binds to G·C sites considerably more weakly than the two dimers, and the methylation of the linker connecting the two pyrazinonaphthalimide units significantly reduces the extent of binding to DNA. There is no doubt that the linker plays an important role in anchoring the drug on DNA. Nevertheless, the sequence selectivity profiles are comparable for the three compounds. The recognition of particular G·C-rich sites appears to be related primarily to the DNA binding ability of the chromophore. In other words, the site selection is essentially governed by the nature of the planar aromatic part of the molecule, not the linker chain. It is instructive to demonstrate that the N-methylation of the alkyl connector has a strong impact on the DNA binding capacity of the drug. This sort of effect may explain, at least partially, why some of the dimeric drugs designed in the aforementioned bisimidazoacridone series do not bind very strongly to DNA and fail to bisintercalate. The antitumor agent WMC26 that contains a $(CH_2)_3N(Me)(CH_2)_3$ linker does not form bisintercalation complexes (*6*, *7*), whereas the corresponding monomer does effectively insert between base pairs. The central *N*-methyl group may well be responsible for the unusual binding property of the dimer. By restricting the molecular contacts between the linker and the sugar−phosphate DNA backbone, the *N*-methyl group may cause the imidazoacridone to fall out of the intercalation site. A similar explanation can be evoked to explain the difficulty of the bisnaphthalimide bisnafide (DMP-80) to form stable complexes with DNA. In this case, the methyl groups are located on the carbon atoms, not the nitrogens (Figure 1), but the steric hindrance is likely comparable. Linker methylation may thus appear to be an easy molecular switch for controlling the degree of drug binding to DNA in these dimer series.

The groove binding issue is a complicated one. As mentioned above, the lead compound elinafide has been found to access DNA via the major groove. Chemical probing experiments and a NMR study concluded that the aminoalkyl side chain of this bisnaphthalimide resides in the major groove of DNA (*29*, *30*), and this is also consistent with other studies with different oligonaphthalimide derivatives (*34*, *35*). Therefore, we expected that the binding of dimer **2** to DNA would be affected by the incorporation of 5-methylcytosine residues in DNA but not by the deletion of the 2-amino group of guanines. The experimental data reported here indicate the opposite behavior in the sense that G → c^7G and C → M substitutions do not impair binding of **2** to DNA, whereas the G → I substitution almost abolishes DNA recognition. At this stage, it is tempting to conclude that the pyrazinonaphthalimide dimer **2** inserts into the minor groove side of the double helix rather than the opposite major groove. However, this is not the only possible explanation. There is not necessarily a direct interaction between the guanine amino group and the drug linker in the DNA minor groove. The reduced affinity of the drugs for the I-containing oligomer may be also a consequence of a reduced level of stacking interactions between the pyrazinonaphthalimide chromophore and the I·C base pairs. The loss of the guanine 2-amino group must lead to much faster breathing motions (base pair opening rates) for the I·C base pair, and this could be responsible for the observed effects in the SPR experiments. Moreover, we cannot also exclude an oligomer folding problem (the inosine substitution destabilizes the double helix which may be folded differently compared to the G oligonucleotide). Additional structural studies will be required to precisely determine the DNA grooves in which the drug linker is located, and this is important from a medicinal chemistry perspective.

In conclusion, we have dissected the DNA sequence selectivity profile of three pyrazinonaphthalimide derivatives. The reversible interaction between dimeric compounds **2** and **3** and DNA has been explored in detail by a complementary SPR−footprinting methodology which optimally combines site selection with accurate DNA affinity analysis. The G·C preference of the drugs has been firmly established, and a high-affinity site encompassing the sequence 5′-GACGGCCAG has been identified. This specific receptor sequence can now be chosen for structural studies by NMR, for example. The comparison of the DNA binding properties of the methylated and nonmethylated compounds also provides useful information for guiding future drug design in this series. In more general terms, the study illustrates that an appropriate combination of a biochemical qualitative method such as DNase I footprinting (the macro

descriptor) and a highly sensitive optical technique such as SPR for quantitative analysis (the micro descriptor) can be useful in better comprehending how small molecules read the genetic information at the heart of the DNA double helix.

ACKNOWLEDGMENT

We thank the IMPRT (IFR114) for access to the BIAcore 3000 instrumentation and Pr. David W. Wilson (Department of Chemistry, Georgia State University, Atlanta, GA) for expert assistance with the SPR experiments.

SUPPORTING INFORMATION AVAILABLE

Three figures showing the DNase I footprinting gels and differential cleavage plots obtained with the 117-mer and 265-mer DNA fragments and the CD spectra of the I- and G-containing hairpin oligonucleotides. This material is available free of charge via the Internet at http://pubs.acs.org.

REFERENCES

1. Le Pecq, J. B., Le Bret, M., Barbet, J., and Roques, B. (1975) DNA polyintercalating drugs: DNA binding of diacridine derivatives, *Proc. Natl. Acad. Sci. U.S.A. 72*, 2915−2919.
2. Wakelin, L. P. G., and Waring, M. J. (1978) Structural limitations on he bifunctional intercalation of diacridines into DNA, *Biochemistry 17*, 5057−5063.
3. King, H. D., Wilson, W. D., and Gabbay, E. J. (1982) Interactions of some novel amide-linked bis(acridines) with deoxyribonucleic acid, *Biochemistry 21*, 4982−4989.
4. Denny, W. A., Baguley, B. C., Cain, B. F., and Waring, M. J. (1983) Antitumour acridines, in *Molecular aspects of anti-cancer drug action* (Neidle, S., and Waring, M. J., Eds.) pp 1−34, Verlag Chemie, Weinheim, Germany.
5. Wakelin, L. P. G. (1986) Polyfunctional DNA intercalating agents, *Med. Res. Rev. 6*, 275−340.
6. Hernandez, L., Cholody, W. M., Hudson, E. A., Resau, J. H., Pauly, G., and Michejda, C. J. (1995) Mechanism of action of bisimidazoacridones, new drugs with potent, selective activity against colon cancer, *Cancer Res. 55*, 2338−2345.
7. Cholody, W. M., Hernandez, L., Hassner, L., Scudiero, D. A., Djurickovic, D. B., and Michejda, C. J. (1995) Bisimidazoacridones and related compounds: New antineoplastic agents with high selectivity against colon tumors, *J. Med. Chem. 38*, 3043−3052.
8. Chaires, J. B., Leng, F., Przewloka, T., Fokt, I., Ling, Y.-H., Perez-Soler, R., and Priebe, W. (1997) Structure-based design of a new bisintercalating anthracycline antibiotic, *J. Med. Chem. 40*, 261−266.
9. Robinson, H., Priebe, W., Chaires, J. B., and Wang, A. H.-J. (1997) Binding of two novel bisdaunorubicins to DNA studied by NMR spectroscopy, *Biochemistry 36*, 8663−8670.
10. Leng, F., Priebe, W., and Chaires, J. B. (1998) Ultratight DNA binding of a new bisintercalating anthracycline antibiotic, *Biochemistry 37*, 1743−1753.
11. Portugal, J., Martin, B., Vaquero, A., Ferrer, N., Villamarin, S., and Priebe, W. (2001) Analysis of the effects of daunorubicin and WP631 on transcription, *Curr. Med. Chem. 8*, 1−8.
12. Spicer, J. A., Gamage, S. A., Rewcastle, G. W., Finlay, G. J., Bridewell, D. J., Baguley, B. C., and Denny, W. A. (2000) Bis-(phenazine-1-carboxamides): structure−activity relationships for a new class of dual topoisomerase I/II-directed anticancer drugs, *J. Med. Chem. 43*, 1350−1358.
13. Deady, L. W., Desneves, J., Kaye, A. J., Finlay, G. J., Baguley, B. C., and Denny, W. A. (2000) Synthesis and antitumor activity of some indeno[1,2-*b*]quinoline-based bis carboxamides, *Bioorg. Med. Chem. 8*, 977−984.
14. Gamage, S. A., Spicer, J. A., Finlay, G. J., Stewart, A. J., Charlton, P., Baguley, B. C., and Denny, W. A. (2001) Dicationic bis(9-methylphenazine-1-carboxamides): relationships between biological activity and linker chain structure for a series of potent topoisomerase targeted anticancer drugs, *J. Med. Chem. 44*, 1407−1415.
15. Mekapati, S. B., Denny, W. A., Kurup, A., and Hansch, C. (2001) QSAR of anticancer compounds. Bis(11-oxo-11*H*-indeno[1,2-*b*]-quinoline-6-carboxamides), bis(phenazine-1-carboxamides), and bis(naphthalimides), *Bioorg. Med. Chem. 9*, 2757−2762.
16. Spicer, J. A., Gamage, S. A., Finlay, G. J., and Denny, W. A. (2002) Synthesis and evaluation of unsymmetrical bis(aryl-carboxamides) designed as topoisomerase-targeted anticancer drugs, *Bioorg. Med. Chem. 10*, 19−29.
17. Cherney, R. J., Swartz, S. G., Patten, A. D., Akamike, E., Sun, J. H., Kaltenbach, R. F., III, Seit, S. P., Behrens, C. H., Getahun, Z., Trainor, G. L., Vavala, M., Kirshenbaum, M. R., Papp, L. M., Stafford, M. P., Czerniak, P. M., Diamond, R. J., McRipley, R. J., Page, R. J., and Gross, J. L. (1997) The synthesis and antitumor evaluaion of unsymmetrical bis-imides, *Bioorg. Med. Chem. Lett. 7*, 163−168.
18. O'Reilly, S., Baker, S. D., Sartorius, S., Rowinsky, E. K., Finizio, M., Lubiniecki, G. M., Grochow, L. B., Gray, J. E., Pieniaszek, H. J., Jr., and Donehower, R. C. (1998) A phase I and pharmacologic study of DMP 840 administered by 24-hour infusion, *Ann. Oncol. 9*, 101−104.
19. Thompson, J., Pratt, C. B., Stewart, C. F., Avery, L., Bowman, L., Zamboni, W. C., and Pappo, A. (1998) Phase I study of DMP840 in pediatric patients with refractory solid tumors, *Invest. New Drugs 16*, 45−49.
20. Bousquet, P. F., Braña, M. F., Conlon, D., Fitzgerald, K. M., Perron, D., Cocchiaro, C., Miller, R., Moran, M., George, J., Qian, X.-D., Keilhauer, G., and Romerdahl, C. A. (1995) Preclinical evaluation of LU 79553: a novel bisnaphthalimide with potent antitumor activity, *Cancer Res. 55*, 1176−1180.
21. Villalona-Calero, M. A., Eder, J. P., Toppmeyer, D. L., Allen, L. F., Fram, R., Velagapudi, R., Myers, M., Amato, A., Kagen-Hallet, K., Razvillas, B., Kufe, D. W., Von Hoff, D. D., and Rowinsky, E. K. (2001) Phase I and pharmacokinetic study of LU79553, a DNA intercalating bisnaphthalimide, in patients with solid malignancies, *J. Clin. Oncol. 19*, 857−869.
22. Pavlov, V., Kong Thoo Lin, P., and Rodilla, V. (2001) Cytotoxicity, DNA binding and localisation of novel bis-naphthalimidopropyl polyamine derivatives, *Chem.-Biol. Interact. 137*, 15−24.
23. Nitiss, J. L., Zhou, J., Rose, A., Hsiung, Y., Gale, K. C., and Osheroff, N. (1998) The bis(naphthalimide) DMP-840 causes cytotoxicity by its action against eukaryotic topoisomerase II, *Biochemistry 37*, 3078−3085.
24. Cobb, P. W., Degen, D. R., Clark, G. M., Chen, S. F., Kuhn, J. G., Gross, J. L., Kirshenbaum, M. R., Sun, J. H., Burris, H. A., and Von Hoff, D. D. (1994) Activity of DMP840, a new bis-naphthalimide, on primary human tumor colony-forming units, *J. Natl. Cancer Inst. 5*, 1462−1465.
25. Houghton, P. J., Cheshire, P. J., Hallman, J. C., Gross, J. L., McRipley, R. J., Sun, J. H., Behrens, C. H., Dexter, D. L., and Houghton, J. A. (1994) Evaluation of a novel bis-naphthalimide anticancer agent, DMP840, against human xenografts derived from adult, juvenile, and pediatric cancers, *Cancer Chemother. Pharmacol. 33*, 265−272.
26. Kirshenbaum, M. R., Chen, S.-F., Behrens, C. H., Papp, L. M., Stafford, M. M., Sun, J.-H., Behrens, D. L., Fredericks, J. R., Polkus, S. T., Sipple, P., Patten, A. D., Dexter, D., Seitz, S. P., and Gross, J. L. (1994) (*R,R*)-2,2′-[1,2-ethanediylbis[imino(1-methyl-2,1-ethanediyl)]]-bis[5-nitro-1*H*-benz[de]isoquinoline-1,3-(2*H*)-dione] dimethanesulfonate (DMP 840), a novel bis-naphthalimide with potent nonselective tumoricidal activity *in vitro*, *Cancer Res. 54*, 2199−2206.
27. McRipley, R. J., Burns-Horwitz, P. E., Czerniak, P. M., Diamond, R. J., Diamond, M. A., Miller, J. L. D., Page, R. J., Dexter, D. L., Chen, S.-F., Sun, J. H., Behrens, C. H., Seitz, S. P., and Gross, J. L. (1994) Efficacy of DMP 840: A novel bis-naphthalimide cytotoxic agent with human solid tumor xenograft selectivity, *Cancer Res. 54*, 159−164.
28. LoRusso, P., Demchik, L., Dan, M., Polin, L., Gross, J. L., and Corbett, T. H. (1995) Comparative efficacy of DMP 840 against mouse and human solid tumor models, *Invest. New Drugs 13*, 195−203.
29. Bailly, C., Braña, M., and Waring, M. J. (1996) Sequence-selective intercalation of antitumour bisnaphthalimides into DNA. Evidence for an approach via the major groove, *Eur. J. Biochem. 240*, 195−208.
30. Gallego, J., and Reid, B. R. (1999) Solution structure and dynamics of a complex between DNA and the antitumor bisnaphthalimide LU-79553: intercalated ring flipping on the millisecond time scale, *Biochemistry 38*, 15104−15115.

31. Neidle, S. (2001) DNA minor-groove recognition by small molecules, *Nat. Prod. Rep. 18*, 291−309.
32. Delbarre, A., Delepierre, M., Garbay, C., Igolen, J., Le Pecq, J. B., and Roques, B. P. (1987) Geometry of the antitumor drug ditercalinium bis intercalated into $d(CpGpCpG)_2$ by ^1H NMR, *Proc. Natl. Acad. Sci. U.S.A. 84*, 2155−2159.
33. Gao, Q., Williams, L. D., Egli, M., Rabinovich, D., Chen, S. L., Quigley, G. J., and Rich, A. (1991) X-ray structure of a DNA-ditercalinium complex, *Proc. Natl. Acad. Sci. U.S.A. 88*, 2422−2426.
34. Lokey, R. S., Kwok, Y., Guelev, V., Pursell, C. J., Hurley, L. H., and Iverson, B. L. (1997) A new class of polyintercalating molecules, *J. Am. Chem. Soc. 119*, 7202−7210.
35. Guelev, V., Lee, J., Ward, J., Sorey, S., Hoffman, D. W., and Iverson, B. L. (2001) Peptide bis-intercalator binds DNA via threading mode with sequence specific contacts in the major groove, *Chem. Biol. 8*, 415−425.
36. Brãna, M. F., Castellano, J. M., Morán, M., Pérez de Vega, M. J., Romerdahl, C. R., Qian, X.-D., Bousquet, P., Emling, F., Schlick, E., and Keilhauer, G. (1993) Bis-naphthalimides: a new class of antitumor agents, *Anti-Cancer Drug Des. 8*, 257−268.
37. Brãna, M. F., Castellano, J. M., Morán, M., Pérez de Vega, M. J., Perron, D., Conlon, D., Bousquet, P. F., Romerdahl, C. A., and Robinson, S. P. (1996) Bis-naphthalimides 3: Synthesis and antitumor activity of N,N′-bis[2-(1,8-naphthalimido)-ethyl]alkanediamines, *Anti-Cancer Drug Des. 11*, 297−309.
38. Brãna, M. F., Cacho, M., Gradillas, A., de Pascual-Teresa, B., and Ramos, A. (2001) Intercalators as anticancer drugs, *Curr. Pharm. Des. 7*, 1745−1780.
39. Wright, R. G. McR., Wakelin, L. P. G., Fieldes, A., Acheson, R. M., and Waring, M. J. (1980) Effects of ring substituents and linker chains on the bifunctional intercalation of diacridines into deoxyribonucleic acid, *Biochemistry 19*, 5825−5836.
40. Brãna, M. F., Castellano, J. M., Moran, M., Emling, F., Kluge, M., Schlick, E., Klebe, G., and Walker, N. (1995) Synthesis, structure and antitumor activity of new benz[*d*,*e*]isoquinoline-1,3-diones, *Arzneim.-Forsch. 45*, 1311−1318.
41. Brãna, M. F., Castellano, J. M., Perron, D., Maher, C., Conlon, D., Bousquet, P. F., George, J., Qian, X. D., and Robinson, S. P. (1997) Chromophore-modified bis-naphthalimides: synthesis and antitumor activity of bis-dibenz[de,h]isoquinoline-1,3-diones, *J. Med. Chem. 40*, 449−454.
42. Sami, S. M., Dorr, R. T., Alberts, D. S., Solyom, A. M., and Remers, W. A. (2000) Analogues of amonafide and azonafide with novel ring systems, *J. Med. Chem. 43*, 3067−3073.
43. Braña, M. F., Cacho, M., García, M. A., Pascual-Teresa, B., Ramos, A., Acero, N., Llinares, F., Muñoz-Mingarro, D., Abradelo, C., Rey-Stolle, M.-F., and Yuste, M. (2002) Synthesis, antitumor activity, molecular modeling, and DNA binding properties of a new series of imidazonaphthalimides, *J. Med. Chem. 45*, 5813−5816.
44. Bailly, C., Carrasco, C., Joubert, A., Bal, C., Wattez, N., Hildebrand, M. P., Lansiaux, A., Colson, P., Houssier, C., Cacho, M., Ramos, A., and Braña, M. F. (2003) Chromophore-modified bis-naphthalimides: DNA recognition, topoisomerase inhibition and cytotoxic properties of two mono- and bis-furonaphthalimides, *Biochemistry 42*, 4136−4150.
45. Braña, M. F., Cacho, M., Ramos, A., Dominguez, M. T., Pozuelo, J. M., Abradelo, C., Rey-Stolle, M. F., Yuste, M., Carrasco, C., and Bailly, C. (2003) Synthesis, biological evaluation and DNA binding properties of novel mono- and bisnaphthalimides, *Org. Biomol. Chem. 1*, 648−654.
46. Davis, T. M., and Wilson, W. D. (2000) Determination of the refractive index increments of small molecules for correction of surface plasmon resonance data, *Anal. Biochem. 284*, 348−353.
47. Davis, T. M., and Wilson, W. D. (2001) Surface plasmon resonance biosensor analysis of RNA-small molecule interactions, *Methods Enzymol. 340*, 22−51.
48. Connors, K. A. (1987) *Binding Constants*. Wiley, New York.
49. Lavesa, M., and Fox, K. R. (2001) Preferred binding sites for [N-MeCys(3),N-MeCys(7)]TANDEM determined using a universal footprinting substrate, *Anal. Biochem. 293*, 246−250.
50. Bailly, C., and Waring, M. J. (1995) Comparison of different footprinting methodologies for detecting binding sites for a small ligand on DNA, *J. Biomol. Struct. Dyn. 12*, 869−898.
51. Wilson, W. D. (2002) Analyzing biomolecular interactions, *Science 295*, 2103−2105.
52. Nguyen, B., Tardy, C., Bailly, C., Colson, P., Houssier, C., Kumar, A., Boykin, D. W., and Wilson, W. D. (2002) Influence of compound structure on affinity, sequence selectivity and mode of binding to DNA for unfused aromatic dications related to furamidine, *Biopolymers 63*, 281−297.
53. Carrasco, C., Facompré, M., Chisholm, J. D., Van Vranken, D. L., Wilson, W. D., and Bailly, C. (2002) DNA sequence recognition by the indolocarbazole antitumor antibiotic AT2433-B1 and its diastereoisomer, *Nucleic Acids Res. 30*, 1774−1781.
54. Wilson, W. D., Wang, L., Tanious, F., Kumar, A., Boykin, D. W., Carrasco, C., and Bailly, C. (2001) BIAcore and DNA footprinting for discovery and development of new DNA targeted therapeutics and reagents, *BIAcore J. 1*, 15−19.
55. Wang, L., Bailly, C., Kumar, A., Ding, D., Bajic, M., Boykin, D. W., and Wilson, W. D. (2000) Specific molecular recognition of mixed nucleic acid sequences: An aromatic dication that binds in the DNA minor groove as a dimer, *Proc. Natl. Acad. Sci. U.S.A. 97*, 12−16.
56. Wang, L., Carrasco, C., Kumar, A., Stephens, C. E., Bailly, C., Boykin, D. W., and Wilson, W. D. (2001) Evaluation of the influence of compound structure on stacked-dimer formation in the DNA minor groove, *Biochemistry 40*, 2511−2521.
57. Lacy, E. R., Le, N. M., Price, C. A., Lee, M., and Wilson, W. D. (2002) Influence of a terminal formamido group on the sequence recognition of DNA by polyamides, *J. Am. Chem. Soc. 124*, 2153−2163.
58. Nguyen, B., Lee, M. P. H., Hamelberg, D., Joubert, A., Bailly, C., Brun, R., Neidle, S., and Wilson, W. D. (2002) Strong binding in the DNA minor groove by an aromatic diamidine with a shape that does not match the curvature of the groove, *J. Am. Chem. Soc. 124*, 13680−13681.
59. Carrasco, C., Vezin, H., Wilson, W. D., Ren, J., Chaires, J. B., and Bailly, C. (2002) DNA binding properties of the indolocarbazole antitumor drug NB-506, *Anti-Cancer Drug Des. 16*, 99−107.
60. Carrasco, C., Rosu, F., Gabelica, V., Houssier, C., De Pauw, E., Garbay-Gaureguiberry, C., Roques, B., Wilson, W. D., Chaires, J. B., Waring, M. J., and Bailly, C. (2002) Tight binding of the antitumor drug ditercalinium to quadruplex DNA, *ChemBioChem 3*, 1235−1241.
61. Teulade-Fichou, M. P., Carrasco, C., Guittat, L., Bailly, C., Alberti, P., Mergny, J. L., David, A., Vigneron, J. P., Lehn, J. M., and Wilson, W. D. (2003) Selective recognition of G-quadruplex telomeric DNA by a bis-quinacridine macrocycle, *J. Am. Chem. Soc. 125*, 4732−4740.

BI034637H